Lasers in Surgery and Medicine 22:240–248 (1998)

Bubble Formation as Primary Interaction Mechanism in Retinal Laser Exposure With 200-ns Laser Pulses

Johann Roider, MD,[1]* El-Sayed El Hifnawi, PhD,[1] and Reginald Birngruber, PhD[2]

[1]Department of Ophthalmology, Medical University of Lübeck, 23568 Lübeck, Germany
[2]Medical Laser Center, 23568 Lübeck, Germany

Background and Objective: **Retinal laser photocoagulation is generally performed by laser pulses of a few hundred milliseconds. The tissue interaction mechanism is a pure thermal interaction mechanism. As pulse duration gets shorter, different, non-thermal interaction mechanisms start to appear. The time domain for a change of tissue interaction mechanism seems to be in the ns and μs range. The goal of this study was to characterize the tissue interaction mechanism with 200-ns laser pulses, which approximate the thermal relaxation time of single melanin granules.**
Materials and Methods: **The retinas of 19 eyes of 10 rabbits were irradiated by 10 and 500 repetitive laser pulses (wavelength, 532 nm; repetition rate, 500 Hz; pulse duration, 200 ns; per pulse energy, 0–120 μJ; retinal spot size, 100 μm). The effects were evaluated by fluorescein angiography, ophthalmoscopy and by theoretical thermal calculations. Light microscopy and transmission electron microscopy were additionally performed on lesions irradiated by 500 pulses.**
Results: **Single pulse threshold energies for angiographic visibility were 3.5 μJ (10 pulses) and 2.1 μJ (500 pulses), for ophthalmoscopic visibility 9.0 μJ (10 pulses) vs. 8.6 μJ (500 pulses). At energy levels above ophthalmoscopic visibility macroscopically visible bubble formation inside the retina could be observed. This occurred at energy levels of 35 μJ (10 pulses) vs. 17 μJ (500 pulses). Microscopic evaluation of lesions irradiated with 500 pulses and energies at the angiographic threshold showed a damage primarily to the RPE. Additional outer segment damage of the photoreceptors could be found. A gap between damaged RPE cells and the outer segments could be repeatedly found as well as damaged RPE cells, which were detached from intact Bruch's membrane. Temperature calculation shows that temperatures above 100°C may exist around single melanin granules.**
Conclusion: **The studies suggest that RPE damage may occur by bubble formation around single melanin granules. Lasers Surg. Med. 22:240–248, 1998.** **© 1998 Wiley-Liss, Inc.**

Key words: bubble; laser; melanin; retina; retinal pigment epithelium

INTRODUCTION

Clinical retinal photocoagulation as performed, for example, in diabetic eyes is generally performed with exposure times of about 100 ms of a green laser, as recommended by the diabetic

*Correspondence to: Johann Roider, MD, Augenklinik, Klinikum Der Universität Regensburg, Franz-Josef-Strauß Allee 11, D-93053 Regensburg, Germany.

Accepted 8 January 1988

retinopathy study research group [1]. The histological observations of damaged choriocapillaris, damaged RPE and photoreceptors after retinal exposure are generally explained by heat diffusion out of the absorbing layer and subsequent thermal denaturation of adjacent tissue. The main absorbing layer with a green laser is the retinal pigment epithelium (RPE), where about 50% of the laser light gets absorbed [2]. General understanding is that the interaction mechanism in retinal photocoagulation with pulse duration longer than 50 ms is a pure thermal mechanism, which can be described by the Arrhenius law [3]. The Arrhenius law basically describes the relationship between tissue temperature and damage observed. The Arrhenius law holds down to the ms range [4]. If the laser pulse duration is shorter several other effects can be found, which no longer can be explained by a pure thermal interaction mechanism. Experiments with Q-switched single ruby laser pulses and energy densities of 45–65 J/cm^2 showed disruptive effects with subsequent bleeding [5,6]. If pulse duration of ps and fs are used pure mechanical effects, like damage produced by stress or shock waves, prevail [7,8]. It is unclear at what pulse duration a change in interaction mechanism from a thermal one to a nonthermal one takes place. It is of special interest what kind of interaction mechanism prevails at the retina, when the laser exposure is in the ns to μs range. Recent experiments with repetitive 5-μs laser exposure have shown that the histological observation after retinal laser exposure with repetitive laser exposures of a green laser (514 nm) could not be explained by a pure thermal mechanism and an additional coexisting mechanism had to be postulated [9]. The order of magnitude of pulse duration, where a change of mechanism could start, can be estimated by the thermal relaxation time of the melanin granules inside the RPE, which are the main absorbers in retinal photocoagulation. Birngruber et al. [4] describes the thermal relaxation time by $t_r = r^2/6\kappa$, where κ is the thermal conductivity of water (1.5×10^{-3} cm^2 s^{-1}) and r the radius. Anderson [10] describe it by $4r^2/27\kappa$. This means that the thermal relaxation time of a single melanin granule with a size of about 0.6 μm [10,11] is on the order of about 100 ns. Therefore laser exposure with pulses in this time domain should show a different interaction mechanism compared to μs or ms laser exposure. Retinal laser exposures in this study were performed with 200 ns pulses (FWHM) of a Nd:YAG (532 nm) laser. To study the interaction mechanism repetitive laser exposures with 10 and 500 laser pulses were applied to the retina. The experimental parameters for retinal laser exposures were—beside the pulse duration—nearly identical to the experimental laser parameters performed earlier [9,12]. In those earlier experiments the parameters were as follows: wavelength 514 nm, pulse duration 5 μs, repetition rate 500 Hz, number of pulses applied between one and 500 pulses, retinal spot size 110 μm, single pulse energy used 2–10 μJ. Therefore it should be possible to make statements on the interaction mechanism with 200 ns laser pulses and to compare it to 5 μs where the interaction mechanism seems to be a primarily thermal one.

MATERIALS AND METHODS

Laser System

A modified prototype of a frequency-doubled Nd:YAG laser (532 nm) (Carl Zeiss GmbH) was used. The pulse duration (FWHM) was 200 ns with a Gaussian shape. The repetition rate was 500 Hz. The number of pulses applied was 10 and 500. The maximum energy available was 120 μJ. The spot size of the laser beam, as analyzed by a beam analyzer (Spicron LBA-100A), was about 160 μm in air. The laser was focused into the animal's eye by a standard laser slitlamp and had a rectangular shape at the retina, since the fiber where the laser was coupled in was imaged to the fundus. A Goldman contact lens was used for all experiments. Detailed calculations show that the measured spot size in air transforms to 100 μm in a rabbit fundus using a plan-concave contact lens [13]. Pulse energy was checked before each experiment by measuring the average power (Scientech MA 100).

Laser Photocoagulation

Nineteen eyes of 10 chinchilla gray rabbits were used, because the density and location of light absorbing pigments in the fundus are rather uniform and similar to that of the human eye. The animals were anesthetized with ketamine hydrochloride (35 mg/kg body weight) and xylazine hydrochloride (5 mg/kg of body weight). The treatment of experimental animals in this study followed both the principles of laboratory animal care as well as the national laws.

Before starting the experimental exposures for orientation a pattern of six to 12 marker lesions was performed to the regio macularis by a conventional cw argon laser (100 ms exposure

TABLE 1. Lesions Investigated Histologically (200 ns, 500 Hz, 500 pulses, 100 μm on the retina)

Energy per pulse	Light microscopy	Transmission electronmicroscopy
2 μJ	8	2
3 μJ	5	2
6 μJ	4	3

TABLE 2. Threshold Energy (ED_{50}) for a Given Effect at 10 and 500 Pulses

	10 pulses (200 ns)	500 pulses (200 ns)
Angiographic visibility	3.5 μJ	2.1 μJ
Ophthalmoscopic visibility	9.0 μJ	8.6 μJ
Bubble formation	≈35 μJ	≈17 μJ
Hemorrhage	not investigated	≈120 μJ

time). The necessary power of these marker lesions varied between 40 and 80 mW. The test lesions to study were performed between the marker lesions and the topographic relationship to the marker lesions was recorded. All test lesions were only performed to the macular region, but not to the periphery. In total 1,170 test lesions were performed. Fundus evaluation was done immediately after exposure by ophthalmoscopy. Fundus evaluation included fluorescein angiography 2 hours after exposure. Fundus pictures were additionally made. Threshold curves for different effects were established by plotting a given effect vs. the necessary single pulse energy. Four end point criteria were investigated: Visibility by fluorescein angiography, visibility by ophthalmoscopy and bubble formation, a new effect which had not been expected.

Morphologic Study

Representative lesions were investigated by light and transmission electron microscopy. The retinas were fixed in 2.5% glutaraldehyde and postfixed in Dalton's osmium fixative, dehydrated in alcohol and embedded in epoxy resin (Epon). Ultrathin sections were stained with uranylacetate. One-micrometer serial sections were cut until the center of the lesions was reached. Seventeen different lesions were investigated by light microscopy and seven different lesions were investigated by transmission electronmicroscopy. All eyes were enucleated in vivo 2 hours after retinal exposure. Table 1 shows the number of lesions investigated. For comparison to the former 5 μs laser lesions in this 200 ns study only lesions after exposure to 500 pulses were examined.

Statistical Analysis

For statistical analysis the incidence of damage visible by fluorescein angiography, ophthalmoscopy and bubble formation was plotted vs. pulse energy for 10 and 500 pulses in a probit plot. The threshold energy ED_{50} is the per-pulse energy necessary to achieve 50% probability of defined damage.

Thermal Calculations

For thermal calculation a thermal model, described earlier [14], was initially used. Since the results of this model showed that the far field of the temperature of the single melanin granules with 200 ns laser pulses can be neglected a pure analytical thermal model for a melanin granule was used. A melanin granule was assumed to have a cylindrical geometry with a diameter of 0.6 μm and a length of 0.6 μm. The analytical solution, described by Vassiliades [15], was used, to calculate the temperature *T:*

$$T(z,t) = \frac{S}{2\rho c}\int_0^t \left(1 - \exp\left[-\frac{a^2}{4az}\right]\right) \left[erf\left(\frac{(z+l)}{2\sqrt{at'}}\right) - erf\left(-\frac{(z-l)}{2\sqrt{at'}}\right)\right] dt' \text{ for } t \leq \tau, \quad (1)$$

where the z is along the axis of symmetry, $2l$ the length of the absorbing cylinder and a the radius of the cylinder. ρ is the density, c the specific heat and α the thermal conductivity and τ the duration of the laser pulse. Thermal properties of water were used. A loss of energy from the cornea to the RPE of 7% was assumed. The total energy absorption of a single melanin granule was assumed by 63%, which is consistent with the total absorption of green light of an RPE layer [9].

RESULTS

Statistical Results

Table 2 shows the statistical results of threshold energy (ED_{50}) necessary to achieve a given effect with the Nd:Yag laser (532 nm) (100 μm spot size on the retina, 500 Hz, 200 ns).

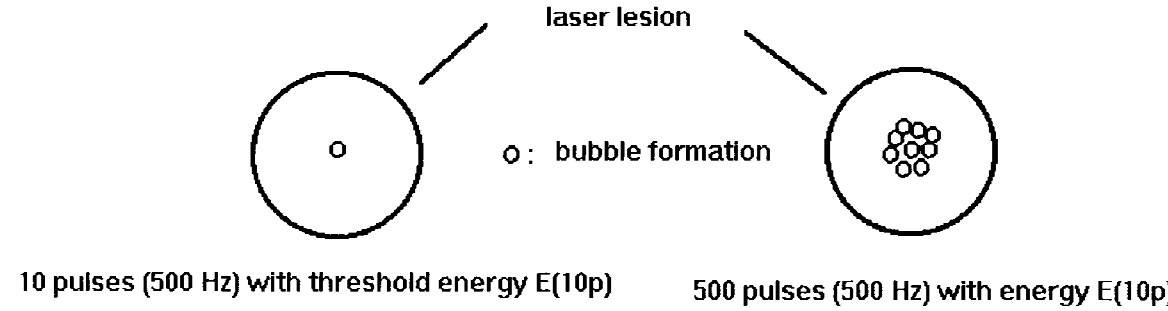

Fig. 1. Schematic drawing of macroscopic visible bubble formation inside a laser lesion after application of 10 and 500 pulses at a repetition rate of 500 Hz. If 10 pulses with single pulse energies at threshold of bubble formation are applied to the fundus a single bubble can be observed in the middle of the chalk-white laser lesion. However, if 500 pulses of the same per pulse energy are used several adjacent bubbles can be seen.

Ophthalmoscopic Results

With increasing energy the lesions become visible by ophthalmoscopy. Initially the lesions appear gray, and later they become white and ultimately chalk white. With increasing energy a phenomena started to appear, which we call macroscopic bubble formation. Initially tiny, reflecting surfaces in middle of the white lesions can be detected and with more energy they appear as a single three-dimensional bubble-like appearance in middle of the lesion. The size of the bubble is energy dependent. It is interesting to note that after application of 500 pulses with energies, which are at the threshold of bubble formation of 10 pulses, several adjacent bubbles start to appear. Figure 1 illustrates this situation. These bubbles were visible more than 1 hour after irradiation. Bleeding always started from the bubbles in middle of the chalk-white lesions. The hemorrhage was a choroidal hemorrhage.

Histology

All lesions investigated by histology were exposed by 500 pulses and 500 Hz. In order to get an idea on the mechanism with 200 ns all lesions investigated were exposed with energy levels at the angiographic threshold ranging between 2 and 6 μJ (25 mJ/cm^2–75 mJ/cm^2). All the lesions were not visible by ophthalmoscopy, only by flourescein angiography.

All the lesions were located primarily to the retinal pigment epithelium (RPE). Melanin granules appear ultrastructurally intact and were apically located at their primary site. No damage could be detected in the choriocapillaris. Bruch's membrane was intact in all cases. Some damage, depending on the energy used, was visible in the photoreceptor layer. No damage was visible to the other inner retinal layers. With 2 μJ energy per pulse the RPE is heavily damaged. The cytoplasm is condensed. Degenerative changes are visible at the directly adjacent outer segments, showing homogeneous, electronlucent discs. The outer segments are often irregularly orientated both inside as well as at the edge of the lesion. With 3 μJ energy per laser pulse the lesion is also confined primarily to the RPE. Regularly a space between the irradiated, damaged RPE and the photoreceptor outer segments could be found (see Fig. 2). RPE cells can be completely lost, so that photoreceptor outer segments approach the underlying morphologically intact Bruch's membrane (see Fig. 3). In several cases the damaged RPE was detached from intact Bruch's membrane showing a space between these two layers (see Fig. 4). Outer segments appear repeatedly shortened. Parts of damaged outer segments could be seen between morphologically intact OS. Occasionally mitochondrias of the inner segments appear vacuolized.

The lesions irradiated by 6 μJ are easily detected by light microscopy. The space between the RPE and outer segments is easy to detect. Outer segments appear irregularly orientated. It is noteworthy that damaged cell nucleoli could be repeatedly found, which showed ultrastructurally normal membrane of the nucleus, while the cell nucleus is condensed and its chromatin is shrunken (see Fig. 5). Damage to the inner segments could be found, showing damaged mitochondria. Occasionally a pycnotic cell nucleus could be found inside the outer nuclear layer.

Temperature Calculations

Figure 6 shows the spatial temperature profile in the immediate neighborhood of a single

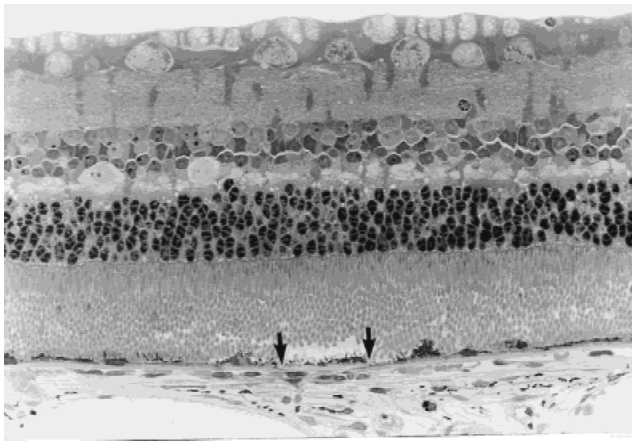

Fig. 2. Light micrograph obtained 2 hours after irradiation (500 pulses, 200 ns, 500 Hz, 3 μJ single pulse energy). The irradiated RPE is completely damaged (arrows). A space between the irradiated RPE and the outer segments can be found (×550).

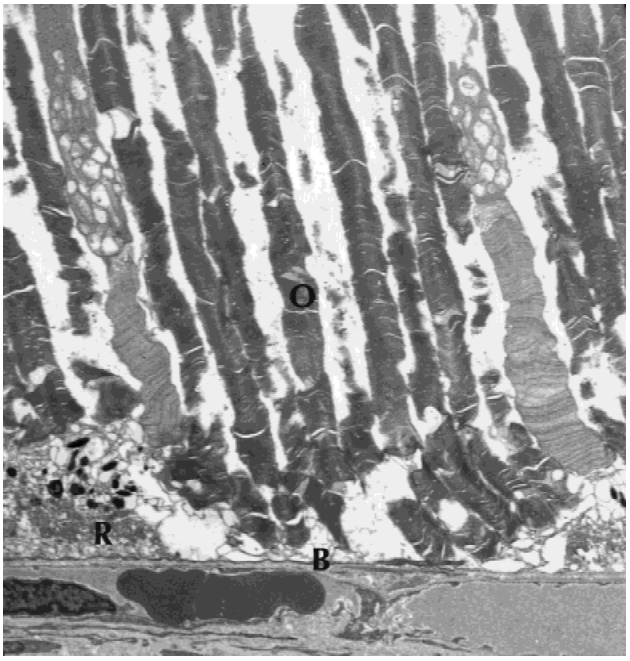

Fig. 3. Transmission electron micrograph obtained 2 hours after pulsed irradiation (500 pulses, 200 ns, 500 Hz, 3 μJ single pulse energy). RPE cells have been completely lost, so that photoreceptor outer segments (O) approach the underlying morphologically intact Bruch's membrane (B). (R: damaged RPE) (×3,780).

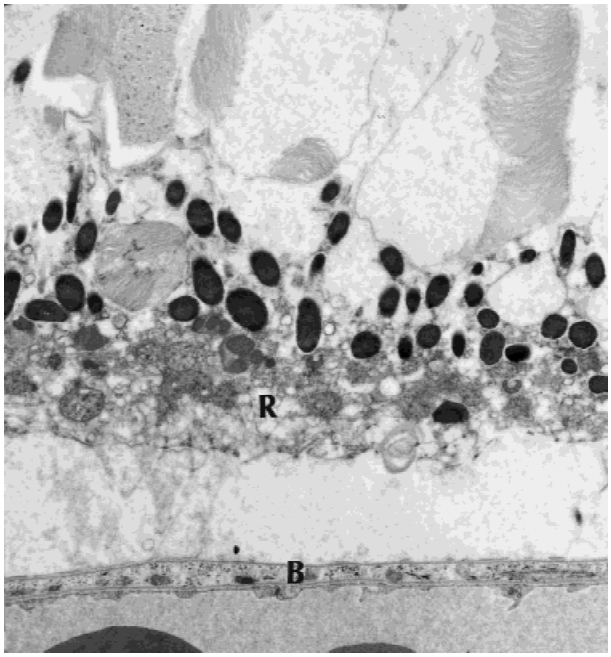

Fig. 4. Transmission electron micrograph obtained 2 hours after pulsed irradiation (500 pulses, 200 ns, 500 Hz, 3 μJ single pulse energy). The RPE is completely damaged. Melanin granules appear normal. The whole damaged RPE (R) is completely detached from the morphologically intact Bruch's membrane (B). (×9,660).

melanin granule at the end of a 200 ns laser pulse and a 5 μs laser pulse using equation 1. At all calculations the same energy ($1.21 \cdot 10^{-10}$ J) was used. The energy used ($1.21 \cdot 10^{-10}$ J) is the energy which hits the cross section of single melanin granule (0.6 μm diameter) inside a rectangular laser spot of 100 μm and a total laser energy of 6 μJ. A single melanin absorption of 63% was used and a loss of energy of 7% from the cornea to the RPE is assumed. It can he seen that there is significant heat conduction out of the granule with e.g. a 5 μs laser pulse, but only little with a 200 ns laser pulse. The adiabatic temperature can be calculated to about 170°C. If 200 ns laser pulses are used the maximum temperature increase is about 125°C at 6 μJ pulse energy due to some heat conduction. Using 3 μJ per pulse energy, exposure parameters as experimentally used, the temperature increase can be calculated to 62.5°C. For the absolute temperatures body temperature of 37°C has to be added. This means that the absolute temperature reaches at least 100°C after each single 200 ns laser pulse of 3 μJ energy and 160°C after 6 μJ energy.

DISCUSSION

In order to elucidate the mechanism the results have to be compared to results published earlier, where also laser exposures have been made to the retina [9,12]. The exposures in those earlier experiments have been made to the retina

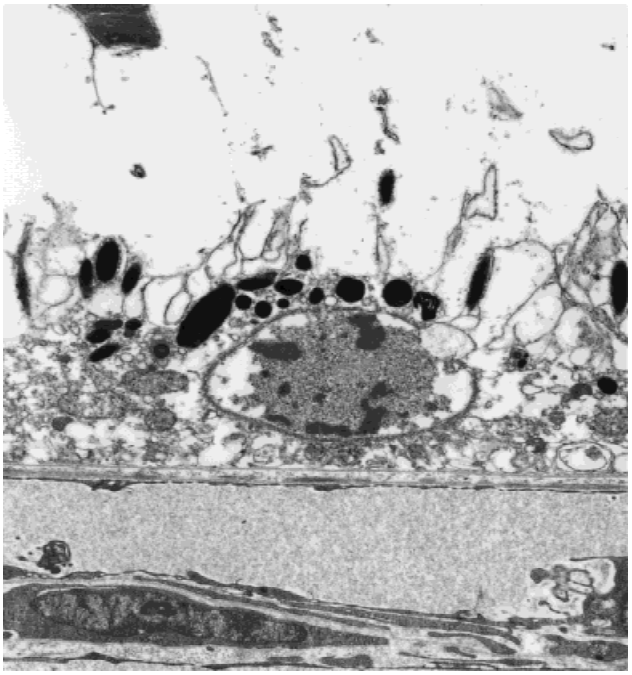

Fig. 5. Transmission electron micrograph obtained 2 hours after pulsed irradiation (500 pulses, 200 ns, 500 Hz, 6 μJ single pulse energy). After irradiation the cell nucleus is condensed and its chromatin is shrunken. The membrane of the nucleus can still be seen. Melanin granules appear morphologically intact. (×8,740).

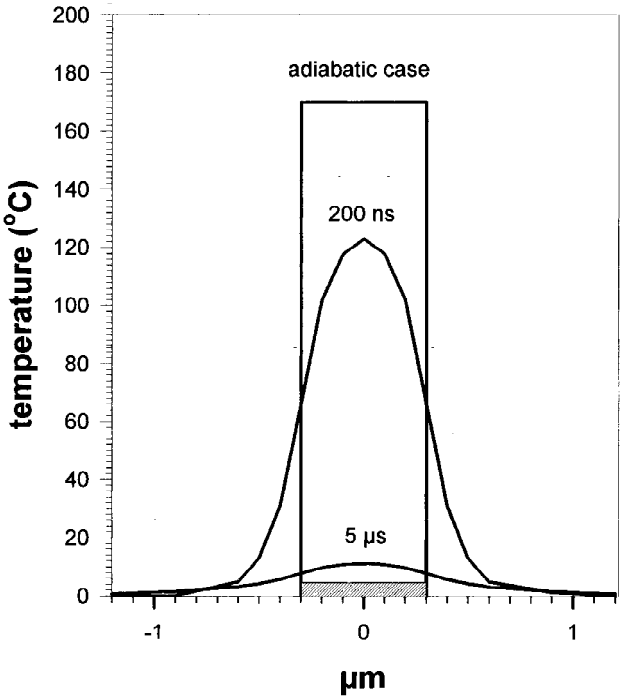

Fig. 6. Temperature profile inside and around a single melanin granule as calculated by using equation 1 after a 5-μs laser pulse and after a 200-ns laser pulse. Each laser pulse contains the same amount of energy of $1.21 \cdot 10^{-10}$ J.

with nearly identical parameters beside the pulse duration. The parameters were as follows: wavelength 514 nm, pulse duration 5 μs, repetition rate 500 Hz, number of pulses applied between one and 500 pulses, retinal spot size 110 μm, single pulse threshold energies for 500 repetitive pulses 1.5 μJ [9,12]. Similarly to the results reported here the RPE was heavily damaged while there was sparing of the photoreceptors. The analysis of these data showed that the primary damage mechanism is a thermal one with an additional, unknown mechanism. In those experiments no histological clues for a primary thermomechanic or acoustic mechanism were found. The observations reported here after exposure with repetitive 200 ns laser pulses show some similarities to those 5 μs experiments but many differences.

In both experimental series some additivity of the effects was found. In Figure 7 the energy density per single pulse is plotted vs. number of pulses applied in a logarithmic scale for those early μs experiments and the 200 ns experiments. The ED_{50} values for a angiographic visible lesion were used. Additionally the ED_{50} values for vessel occlusion for arterioles and venules for repetitive laser pulses with 160 μs laser pulses were plotted as well [16]. In those 160 μs experiments arterioles and venules of 30 μm diameter of the hamster cheek pouch were irradiated with a pulsed dye laser (577 nm, 160 μs, 1.2 mm spot size, 0.5 Hz) and different number of laser pulses (1, 10 and 100) and vessel occlusion was chosen as an endpoint. Threshold values for vessel occlusion were established. In those 160 μs experiments a thermal mechanism was also shown. In all experiments with repetitive laser exposures a linear relationship can be detected. The relationship can be described by

$$\frac{E(N)}{E_1} = c \cdot N^r, \tag{2}$$

where E_1 is the energy necessary of a single pulse and $E(N)$ the single pulse energy, if N pulses are used. However the correlation factor r is different. In the experiments where the mechanism is supposed to be a primary thermal one the correlation factor r is between −0.19 and −0.22, as opposed to a factor r of −0.13 with the 200 ns laser exposures. This difference in correlation factors could be a hint to a different mechanism.

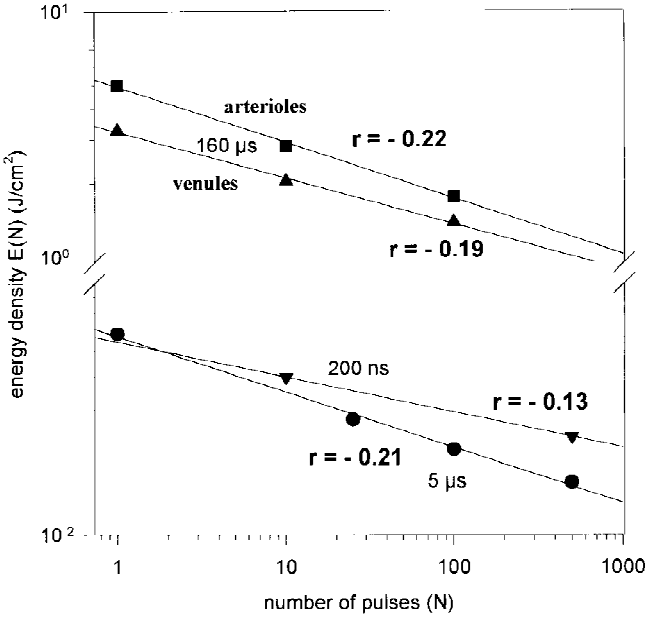

Fig. 7. Threshold energy density vs. number of laser pulses at different pulse durations. The threshold energies for 5 μs are derived from Roider et al. [9] and represent the threshold energies for angiographic visibility. The threshold energies for 160 μs are derived from Roider et al. [16] and represent the threshold values for occlusion of venules and arterioles. The threshold energies for 200 ns represent the current experiments for angiographic visibility. Note that the correlation factor *r,* which describes the dependence between energy necessary for multiple pulses vs. a single pulse (see text), is on the order of –0.2 where a thermal mechanism seems to prevail, as opposed to a factor of –0.13 where a pure mechanical mechanism seems to prevail.

Macroscopic observations after 200 ns laser exposures showed retinal bubble formation with energy densities of about 0.45 J/cm^2 and 10 pulses 0.22 J/cm^2 and 500 pulses. The macroscopic visible bubbles were located inside or below the neural retina, as judged by ophthalmoscopy. Macroscopic bubble formation was also described with a quasi-cw Nd:YAG laser (532 nm) at rabbits and in patients [17] with energy densities of 0.48 J/cm^2. The repetition rate in that laser was 13 kHz and the pulse duration varied due to bad pulse shape irregularly between 1 and 10 μs. This energy density is very similar to our results where macroscopic bubble formation was found with 200 ns pulse duration. This could mean that bubble formation is a phenomenon associated with repetitive short laser pulses.

The energy densities, where angiographic visible lesion could be achieved with the repetitive 200 ns laser pulses, were very similar to the repetitive 5 μs laser pulse experiments. Threshold values for angiographic visibility with 5 μs laser pulses were 5.5 μJ for one pulse, 2.6 μJ for 25 pulses and 1.5 μJ for 500 pulses [12]. However histological analysis showed many differences, which could not be found after irradiation with repetitive 5-μs laser pulses. After 200-ns threshold laser exposures in many lesions a gap between both the damaged RPE and the underlying Bruch's membrane could be found (see Fig. 4). Such effects, like detached RPE cells, had also be found after ps laser exposures [18]. In several lesions a gap between the RPE and the photoreceptors could be found (see Fig. 2). The outer segments were orientated irregularly after laser exposures and appeared shorter compared to non-irradiated areas. All such effects could never be found after repetitive 5-μs laser exposures. RPE cells can be completely lost, so that photoreceptor outer segments approach the underlying morphologically intact Bruch's membrane (see Fig. 3). Inner segments showed some damage after irradiation with higher laser energy (6 μJ). Compared to the experiments with the repetitive 5-μs laser pulses the area of damage is larger and the damage mechanism seems to be different.

The primary interaction mechanism after irradiation with 200-ns laser pulses seems to be a non-thermal mechanism. If one assumes that tissue damage takes place inside the RPE cell, maybe a few μm away from the melanin granules, the absolute temperatures are much too low to explain the histological effects by a thermal mechanism. Generally all authors agree that no thermal effect takes place with laser pulses in the ns range. Melanin can oxidize different cell components like vitamin C [19]. Therefore a photochemical mechanism has also to be considered. However reactivity of melanin strongly depends on the intact structure, as shown with experiments of 10-ns pulses of a Nd:YAG (532 nm) [20]. Therefore a photochemical mechanism seems unlikely, since all melanin granules appear intact in our experiments. Lin and Kelly [8] showed by high speed photography shock and stress waves with 100 ps (1,064 nm) and energy densities of 1 J/cm^2. Morphological signs for a pure acoustic damage like dilated endoplasmatic reticulum were not found [21]. Furthermore the retinal energy densities in our experiments are much too low to create such effects. Energy densities at angiographic threshold are between 0.025 and 0.075 J/cm^2.

Temperature calculations showed that no cumulative temporal temperature effects due to repetitive laser pulse exposures exist, because the

repetition rate is only 500 Hz [14]. Therefore it is sufficient to consider the temperature profile after a single laser pulse. The temperature calculations show that absolute temperatures of at least 100°C to 160°C may prevail in the energy range where histological examination was performed (3–6 μJ respectively 0.04–0.08 J/cm^2). This temperature profile is basically built up every 2 ms, because the repetition rate is 500 Hz. Each single melanin granule has neighboring melanin granules, which could additionally contribute to the real temperature profile of the granule of interest, since there is some small heat conduction. A comparison of the analytical results of the multiple granule model [14] shows that the real temperature profile of a single melanin granule surrounded by neighboring melanin granules with an average distance of 1.2 μm in the RPE is not higher than 30% than the temperature due to single absorption of a single granule [14]. The distance of 1.2 μm is the average distance of melanin granules inside the RPE [13]. Therefore it is reasonable to consider only the temperature profile around a single melanin granule. As summary the temperature calculations show that the temperatures inside the melanin granules exceed 100°C with 3 and 6 μJ pulse energy (0.04 and 0.08 J/cm^2). The absolute temperatures are completely different to those prevailing e.g. after a single 5-μs laser pulse, where significant heat conduction out of a single melanin granule occurs. At energy densities of 0.22 J/cm^2, where macroscopic bubble formation regularly appears with 200 ns, temperatures far beyond 100°C prevail. Theoretically Hansen and Fine [22] thought that steam formation around melanin granules around single melanin granules may take place. Gerstman [23] postulated a similar mechanism and tried to correlate the size and energy necessary for bubble formation by analytical analysis. Depending on the absorption of the melanin granules they predict energy densities between 0.73 J/cm^2 and 1.23 J/cm^2, which may lead to bubble formation. These bubbles should have a size of about 10 μm. These values are close to our experimental values, where macroscopic visible bubble formations have been detected. The fact that with 10 pulses only a single tiny bubble was found, but with 500 pulses and identical energy several adjacent bubbles appear, is consistent with the theory of bubble formation inside the RPE. Gerstman [23] postulated that bubble formation can take place even at lower energies, but such situations cannot be analytically calculated. Our experiments show many signs which are consistent with the assumption that even at lower energies bubble formation around single melanin granules may act as primary interaction mechanism. A space between the RPE and Bruch's membrane as well a gap between the RPE and the outer segments was repeatedly found. Additionally irregularly orientated outer segments were repeatedly found. Also the fact that even 2 hours after irradiation the cell nucleus still shows a membrane structure and is not homogeneously coagulated is not consistent with a pure thermal coagulation mechanism. All these findings could be explained by bubble formation around single melanin granules. It may be that even damaged RPE cells could be pushed apart, as found by TEM (see Fig. 3). It is unclear whether damage takes place only inside the bubble or outside such a bubble as well. The altered and disorientated outer segments could be a hint that damage may take place even outside the bubble. The histological findings of the altered outer and inner segments could be explained e.g. by compression outside of the bubble.

In summary all findings found in these experiments do not support a primary thermal coagulation mechanism. Both the macroscopic findings, the histological findings as well as the threshold values and the temperature calculations are consistent with the theory of a primary bubble formation interaction mechanism.

REFERENCES

1. The Diabetic Retinopathy Study Research Group. Report no. 8. Invest Ophthalmol Vis Sci 1981; 88:583.
2. Gabel V-P, Birngruber R, Hillenkamp F. Visible and near infrared light absorption in pigment epithelium and choroid. In: Shimizu K, Oosterhuis JA, eds. Internat Congr Series No. 450, XXIII Concilium Ophthalmologicum, Kyoto. Amsterdam, Oxford: Excerpta Medica, pp 658–662.
3. Arrhenius S. Über die Reaktionsgeschwindigkeit bei der Inversion von Rohrzucker durch Säuren. Z Phys Chem 1889; 4:226–248.
4. Birngruber R, Hillenkamp F, Gabel V-P. Theoretical investigations of laser thermal retinal injury. Health Phys 1985; 48:781–796.
5. Marshall J. Thermal and mechanical mechanisms in laser damage to the retina. Invest Ophthalmol 1970; 9:97–115.
6. Marshall J, Mellerio J. Histology of retinal lesions with Q-switched lasers. Exp Eye Res 1968; 7:225–230.
7. Birngruber R, Puliafito CA, Gawande A, Wei-Zhu L, Schoenlein RW, Fujimoto J. Femtosecond laser-tissue interactions: Retinal injury studies. IEEE J Quantum Electr 1987; QE-23:1836–1844.
8. Lin CP, Kelly MW. Ultrafast time-resolved imaging of

stress transient and cavitation from short pulsed laser irradiated melanin particles. Proc SPIE 1995; 2391A: 294–299.
9. Roider J, Hillenkamp F, Flotte T, Birngruber R. Microphotocoagulation: Selective effects in biological tissue using repetitive short laser pulses. Proc Natl Acad Sci USA 1993; 90:8643–8647.
10. Anderson RR, Parrish JA. Selective photothermolysis: Precise microsurgery by selective absorption of pulsed radiation. Science 1983; 220:524–527.
11. Feeney L, Grieshaber JH, Hogan MJ. Studies on "human ocular pigment." In: Rohen JW, ed. "The Structure of the Eye." Stuttgart: Schattauer-Verlag.
12. Roider J, Michaud N, Flotte T, Birngruber R. Response of the RPE to selective photocoagulation of the RPE by repetitive short laser pulses. Arch Ophthalmol 1992; 110: 1786–1792.
13. Birngruber R, Gabel V-P, Hillenkamp F. Experimental studies of laser thermal retinal injury. Health Phys 1983; 44:519–531.
14. Roider J, Birngruber R. Solution of the heat conduction equation. In: Welch AJ, van Gemert M, eds. "Optical-Thermal Response of Laser Irradiated Tissue." New York: Plenum, pp 385–409.
15. Vassiliades A. Ocular damage from laser radiation. In: Wolbarsht ML, ed. Laser Applications in Medicine and Biology. Vol 1. New York, London: Plenum, pp 125–162.
16. Roider J, Schiller M, El-Hifnawi E, Birngruber R. Retinale Photokoagulation mit einem frequenzverdoppelten Nd-Yag-Laser (532 nm). Ophthalmologe 1994; 91:777–782.
17. Roider J, Traccoli J, Michaud N, Flotte T, Anderson, Birngruber R. Selektiver Gefäßverschluß durch repetierende Laserpulse. Ophthalmologe 1994; 91:274–279.
18. Goldmann AI, Ham WT, Mueller HA. Ocular damage threshold and mechanisms for ultrashort pulses of both visible and infrared laser radiation in the rhesus monkey. Exp Eye Res 1977; 24:45–56.
19. Glickman RD, Lam KW. Oxidation of ascorbic acid as an indicator of photooxidative stress in the eye. Photochem Photobiol (Engl) 1992; 55:191–196.
20. Glickman RD, Jaques SL, Schwartz JA, Lam KW, Buhr G. Photochemical reactivity of RPE melanosomes is increased after disruption by pulsed laser exposures. Invest Ophthalmol Vis Sci 1996; 37 (Suppl.):375.
21. Doukas AG, Flotte TJ. Physical characteristics and biological effects of laser-induced stress waves. Ultrasound Med Biol 1996; 22:151–164.
22. Hansen WP, Fine S. Melanin granule models for pulsed laser induced retinal injury. Appl Optics 1968; 7:155–159.
23. Gerstman BS, Thompson CR, Jaques SL, Rogers ME. Laser induced bubble formation in the retina. Lasers Surg Med 1996; 18:10–21.